Effectiveness of partial wrapping of stainless-steel wire mesh on compression behavior of concrete cylinders

Sunil D Raiyani, Paresh V Patel
Civil Engineering Department, Nirma University, Gujarat, India
sunil.raiyani@nirmauni.ac.in, http://orcid.org/0000-0002-1287-1191
paresh.patel@nirmauni.ac.in, http://orcid.org/0000-0002-2946-2212

S Suriya Prakash
Civil Engineering Department, Indian Institute of Technology Hyderabad, Telangana, India
suriyap@ce.iith.ac.in, http://orcid.org/0000-0003-0319-1773

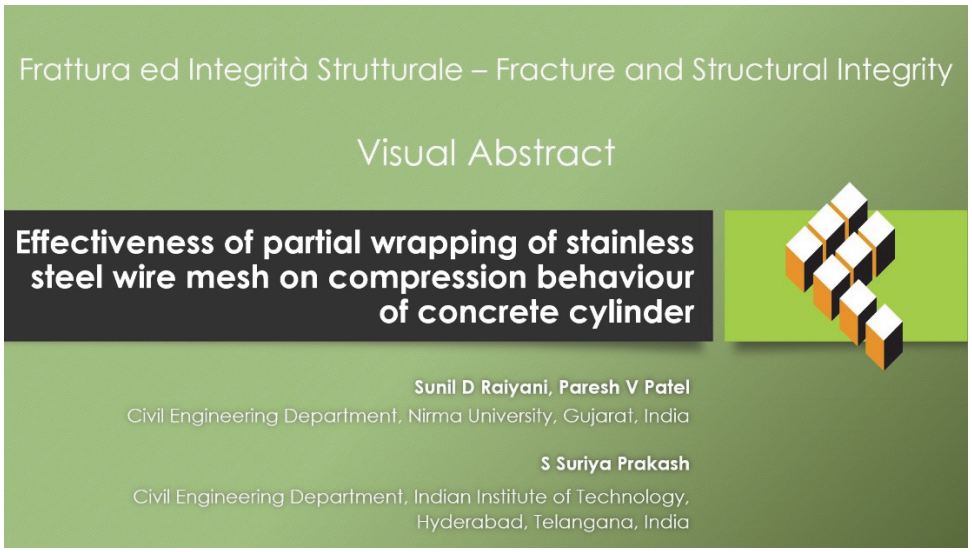

Citation: Raiyani, S. D., Patel, P. V., S Suriya Prakash, Effectiveness of partial wrapping of stainless steel wire mesh on compression behavior of concrete cylinders, Frattura ed Integrità Strutturale, 69 (2024) 71-88.

Received: 31.01.2024
Accepted: 08.04.2024
Published: 20.04.2024
Issue: 07.2024

KEYWORDS. Compression behaviour, Partial wrapping, Stainless Steel Wire Mesh, Concrete cylinder, Confinement coefficient.

INTRODUCTION

Fiber Reinforced Polymer (FRP) composites are commonly used to strengthen concrete structures due to high strength-to-weight ratio, ease of installation and corrosion resistance. Various types of FRP composites, such as glass fibre-reinforced polymer (GFRP), carbon fibre-reinforced polymer (CFRP), and armid fibre-reinforced polymer (AFRP), are being used as strengthening materials. Jahami et al. [1, 2] studied numerically the effect of using CFRP as a strengthening technique for Reinforced Concrete (RC) beams subjected to blast loading. The authors found that using

CFRP enhances load carry capacity and energy absorption as well as reduces central deflection and tensile strain of reinforcements. Stainless Steel Wire Mesh (SSWM) has recently been explored as an alternative to FRP to strengthen concrete structural elements. As SSWM is a locally available material at a lower cost as compared to FRP, strengthening of concrete structures using SSWM will prove to be cost-effective. Wrapping of FRP and SSWM around concrete cylinder provides effective confinement and enhances compressive strength. Numerous studies have been conducted on the compressive behaviour of concrete cylinders partially confined using FRP composites. The CFRP, GFRP, and AFRP composites effectively enhanced the compressive strength and ductility of concrete cylinders. The CFRP-confined concrete cylinders had the highest strength and ductility, followed by AFRP and GFRP-confined concrete cylinders [3, 4]. Wang et al. [5] tested circular concrete cylinders confined with CFRP sheets. They found that the peak compressive strength of the cylinders increased with an increase in the number of CFRP layers, and the failure mode shifted from splitting to crushing with an increase in the gap of the unconfined region. The confinement effectiveness decreased with an increase in the gap of the unconfined region. In addition to the type of FRP and amount of FRP composite, the spacing of the FRP strips has also been found to affect the compressive behaviour of partially confined concrete cylinders. Xiao and Wu [6] investigated the effect of confinement ratio on the compressive behaviour of concrete cylinders wrapped with CFRP, besides the effect of the number of FRP layers. The authors found that the ultimate strength and strain increased with an increase in the number of CFRP layers, but the increase was not directly proportional. They also observed that the confinement effectiveness decreased with the increased unconfined concrete region. The authors suggested the optimal confinement ratio for partially wrapped cylinders between 0.2 and 0.3. The confinement coefficient is varying for different materials [7,8,9,10,11,12]. Based on experimental evidence, Iyengar et al. [10] demonstrated the effectiveness of steel spiral confinement when their pitch was less than least lateral dimension of a normal-strength concrete cylinder. Martinez et al. [11] showed the same behaviour for spirals steel cord confined high-strength concrete. A confinement coefficient in terms of a linear relationship $(1-p_s/2r)$ is suggested, where 'p_s' is the spacing between two spirals of steel cord, and r represents the radius of a concrete cylinder. However, different researchers [13,14,15,16,17,18] suggested that the strength is not directly related to the $p_s/2r$ ratio for confined concrete. As a result, the confinement effectiveness coefficient predicted by Martinez et al. [11] was erroneous. Sheikh and Uzumeri [12] considered the parabolic arching action to separate the two adjacent confined and unconfined concrete portions. A confinement coefficient $(1-p_s \tan\beta/4r)^2$ for concrete confined by steel spirals was suggested based on this assumption. Regression analysis was carried out on experimental results to calculate arched angle β as 45°. The arched angle β can greatly impact the coefficient when concrete is enclosed with diagonal confinement. After observing the experiments and reviewing the literature, it is recommended that the arch action be adapted for partially FRP-confined concrete. Several models have been suggested to predict the strength and ductility of partially FRP-confined cylinders, considering the different parameters that affect the arching action [16,19,20]. However, fewer experimental results are available in the past literature for strengthening concrete cylinders using SSWM. Kumar and Patel [21,22] first attempted to strengthen the circular concrete column with SSWM by keeping variables such as the grade of concrete, the height of the specimen and the number of wraps. However, the literature is silent when discussing the confinement effectiveness coefficient to express the behaviour of SSWM confined concrete cylinders.

The present study analyses the effectiveness of partial wrapping of SSWM on concrete cylinders under compressive loading. As the efficiency of confinement of concrete is maximum in cylindrical specimens, in the present study cylindrical concrete specimens are considered. An experimental program is conducted to understand the behaviour of partially SSWM-confined concrete with changes in the unconfined concrete region between SSWM strips. Then, the axial compressive strength, as well as the axial and hoop strain behaviour of both the wrapped and unwrapped region of the concrete cylinder, is investigated. The strain localisation is studied based on the failure pattern. Based on the present experimental data, an effective confinement coefficient is proposed for estimating the compressive strength of partially SSWM-confined concrete.

Experimental Program

The experimental program includes the evaluation of the material properties, preparation of test specimens, test setup, and Instrumentation to measure the response of specimen during an experiment.

Material properties and specimens' preparation

The axial compression load is applied on eighteen concrete cylindrical specimens with dimensions of 150 mm in diameter and 300 mm in height. According to Indian Standard IS 10262-2019 [23], a concrete mix design of M25 grade is prepared. The various materials of the concrete mix are tested individually as per relevant standards before being used in the mix

design. The proportion of various constituents used to prepare specimens is shown in Tab. 1. As per Indian Standard IS 516 -2021 [24], three cylinders are tested to measure the concrete compressive strength. The average compressive strength of the cylinder at 28 days of curing is achieved as 34.52 MPa.

Material	Cement	Aggregates		Water	Plasticizer
		Fine	Coarse		
Quantity (kg/m^3)	339.54	865.62	1031.96	169.77	2.24
Proportion	1.0	2.6	3.0	0.5	0.007

Table 1: Mixture Design for M25 grade of concrete.

The SSWM is chosen for strengthening cylinders as it can provide better ductility and bonding behaviour with concrete materials while using Sikadur 30LP as compared to other strengthening materials [21,25,26,27]. The plain weave SSWM manufactured from stainless steel of grade SS304 with a square opening of 0.365 mm is considered for the present study. The wire diameter of 40 (mesh per inch) × 32 (standard wire gauge) SSWM measured using the screw gauge is 0.27 mm [28]. The mechanical properties of SSWM, such as modulus of elasticity and the tensile strength, are obtained through coupon tensile test according to ASTM D3039/D3039M [29] and reported by Kumar and Patel [21], Patel et al. [25,30] and Raiyani et al. [26,27]. Three coupons of SSWM 40 × 32 sizes of 25 mm × 175 mm are prepared based on the shape and size provided in ASTM D3039/D3039M [29] as shown in Fig. 1, and actual specimens are shown in Fig. 2. The coupons are cut from the SSWM sheet, and prior to testing, aluminium flat plates are attached at free ends of 25 mm wide coupons as represented in Fig. 2, to reduce the premature failure of SSWM from supports during testing. The SSWM coupons are tested using an Instron Testing machine of 30 kN with mechanical grips, as shown in Fig. 3, at the CASTCON laboratory of IIT Hyderabad. The test is conducted at a rate of 1.27 mm/min in a displacement control mode. The stress-strain characteristics of SSWM samples are depicted in Fig. 4 and Tab. 2. The SSWM coupons began to crack at the stress level, reaching ~ 450.88 MPa at the top near the support section with corresponding strain 0.00227 mm/mm, and failed at ~ 700.16 MPa.

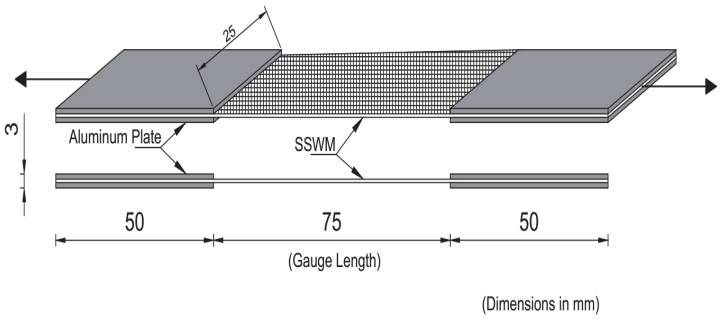

Figure 1: Schematic View of Tensile test coupon of SSWM 40 × 32.

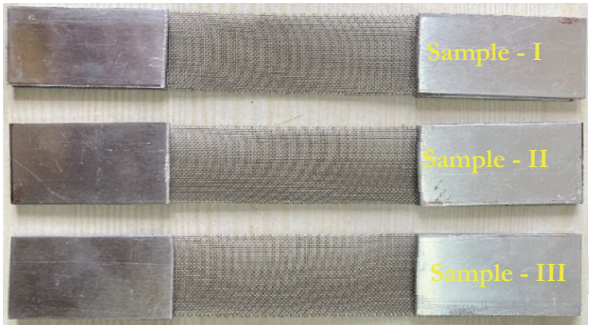

Figure 2: Actual tensile test coupons of SSWM 40 × 32.

For simplicity, the tensile stress-strain curve of SSWM is modelled by two straight lines. To develop a bi-linear representation of the stress-strain curve, average experimental results of stress-strain are considered, as shown in Fig. 4. The first straight line represents the elastic range with a slope of E_{ss}. The second straight line represents the plastic range. These two straight lines intersect at the yield stress (f_{yss}) value. Relevant experimental results of tensile tests on the SSWM based on a bi-linear curve are given in Fig. 5, and corresponding equations for these two straight lines are given in Eqn. 1 and 2. The characteristics of the SSWM can be described using the bi-linear stress-strain curve in the analytical model and finite element (FE) simulation.

$$f_{ss} = E_{ss}\,\varepsilon_{ss} \qquad for \quad \varepsilon_{ss} \le \varepsilon_{yss} \tag{1}$$

$$f_{ss} = 2328.3\varepsilon_{ss} + 445.6 \qquad for \quad \varepsilon_{ss} > \varepsilon_{yss} \tag{2}$$

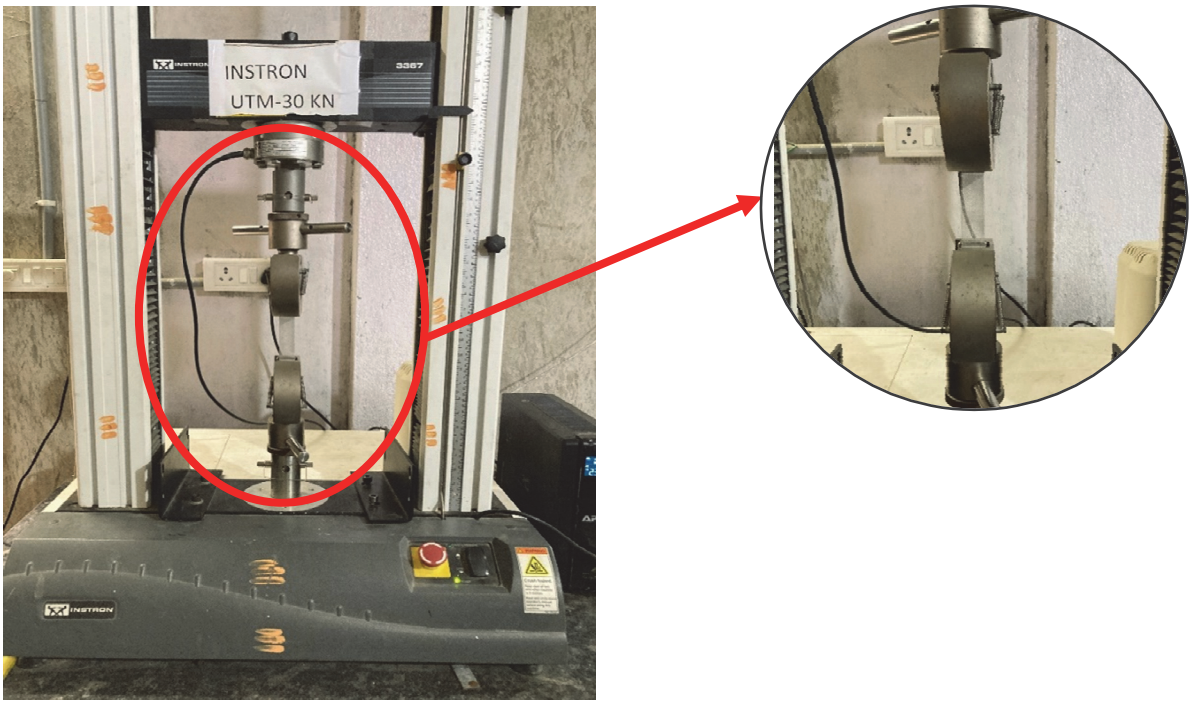

Figure 3: Test setup for tensile test on SSWM 40 × 32.

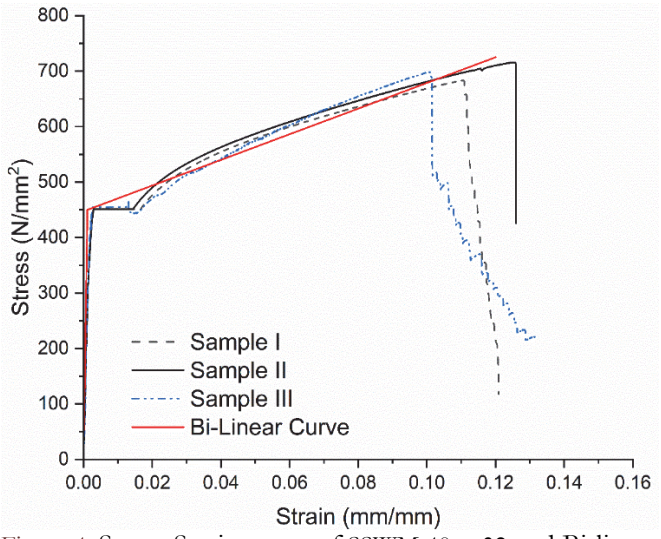

Figure 4: Stress-Strain curve of SSWM 40 × 32 and Bi-linear curve.

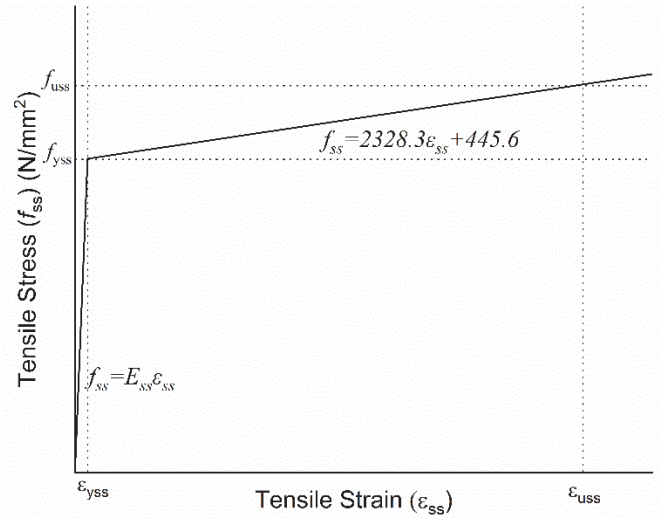

Figure 5: Bi-linear stress-strain curve for SSWM.

The composite used for strengthening concrete cylinders comprises Stainless Steel Wire Mesh (SSWM) and Sikadur 30LP bonding material. Kumar and Patel [21] considered MasterBrace 3500/4500 and Sikadur 30 LP epoxy for bonding SSWM on concrete surfaces. They found higher bond strength with Sikadur30LP as compared to MasterBrace 3500/4500. Further, no debonding of SSWM was observed with Sikadur30LP, and SSWM tore at maximum load. While SSWM was debonded from the concrete surface when MasterBrace 3500/4500 was used to apply SSWM on the concrete surface. So, for utilisation of the full tensile strength of SSWM without debonding from the concrete surface, the authors recommended the use of Sikadur 30 LP as an adhesive to bond SSWM on the concrete surface. Sikadur 30LP is an epoxy resin and hardener combination with a long pot life, does not shrink during hardening, and has good adhesion between SSWM and concrete surfaces [31]. The properties of Sikadur 30LP, as supplied by the manufacturer, are shown in Tab. 3. Before applying the SSWM composite to a concrete cylinder, conducting a bond test between the SSWM and the concrete surface is essential. The double shear lap bond test is used for this purpose, as reported by previous studies [21,25,26,27]. During the bond test,

failure is observed due to wire mesh tearing, and no SSWM debonding occurred. The 40 × 32 type SSWM and Sikadur 30LP epoxy are selected for strengthening the concrete cylinder based on the results of tensile and bond tests [21,25,26,27]. The volumetric ratio (ϱ_s) of SSWM is kept varied to understand the effect of the gap between the confining strips and the effectiveness of SSWM on the partial confinement. Different levels of SSWM confinement are considered, including fully SSWM-wrapped concrete cylinders and partial SSWM-wrapped concrete cylinders having unconfined regions at the centre of the specimens. Gaps between SSWM strips are kept as 30 mm, 60 mm, 90 mm, 120 mm, 150 mm, 180 mm and 210 mm. The detailed SSWM wrapping configurations, along with notations, are shown in Fig.6. Two identical cylindrical concrete specimens are tested for each wrapping configuration.

SSWM Type	40 × 32			Average	Standard Deviation
Specimen	Sp.1	Sp.2	Sp.3		
Width of mesh (mm)	25	25	25		
Diameter of wire (mm)	0.27	0.27	0.27		
Numbers of wires	28	29	28		
c/s area of wire (mm^2)	0.057	0.057	0.057		
Total c/s area mesh (mm^2)	1.60	1.66	1.60		
Yield Strength (MPa)	448.43	450.85	452.88	450.88	1.81
Ultimate Load (N)	1095.05	1189.06	1119.66		
Ultimate tensile strength of Mesh (MPa)	684.41	716.30	699.80	700.16	13.02
Strain at Rupture (ε_{uss}) (mm/mm)	0.126	0.123	0.132	0.127	0.37
Young's Modulus (GPa)		198.95			

Table 2: Mechanical properties of the SSWM 40 × 32.

Property of epoxy	Details
Mixing proportion	3(Resin white in color): 1(Hardener black in color)
Compressive strength	>85 MPa in 7 days
Flexural Tensile strength	>25 MPa in 7 days
Bond Strength	Tensile adhesive strength > 2.5 MPa in 1 day > 18 MPa in 3 days
Pot life of epoxy	60 minutes at ambient temperature
Curing time of epoxy	Ambient curing for 7 days

Table 3: Properties of adhesive Sikadur 30LP as per the manufacturer's specifications [31].

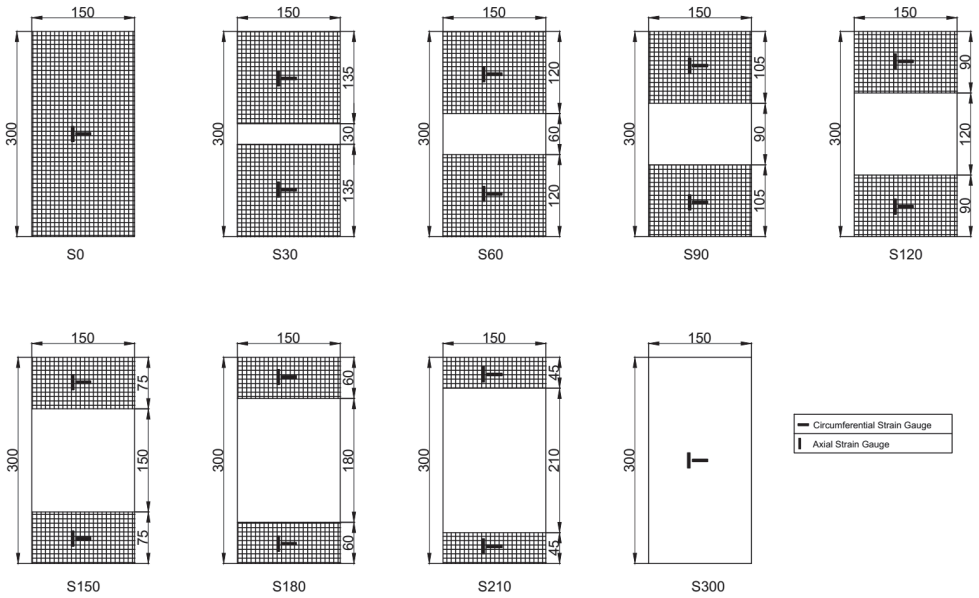

Figure 6: Wrapping configuration on the cylindrical specimen and notations (All dimensions are in mm).

Strengthening procedure

A step-by-step strengthening procedure is performed to wrap SSWM on the surface of the concrete cylinder with the help of bonding epoxy material Sikadur 30 LP, as shown in Fig. 7. Concrete cylinders are kept for 24 hrs surface dry after proper 28 days of wet curing. Before wrapping the SSWM strip, surface grinding of the concrete cylinder is performed for a smooth surface without any honeycombs and loose material, as shown in Fig. 7(a). The dust and dirt from the surface of the cylindrical specimen are removed with the help of an air blower. Then, a strip is tailored from the SSWM roll as per the required wrapping configurations. SSWM wire along the tailored edge should not be damaged while cutting the SSWM strip from the SSWM roll. Marking on the concrete cylinder is made to apply SSWM. The resin and hardener of Sikadur 30LP are blended in a 3:1 ratio for about three minutes with a slow-speed stirrer till the epoxy converts to a uniform grey colour and is consistent. The Sikadur 30LP is applied first on the concrete cylinder surface with nearly 2 mm thickness using a steel plate, as shown in Fig. 7(b). The required size of the SSWM strip is cut before being placed on the recently applied Sikadur 30LP epoxy and gently pressed to achieve correct alignment and installation without air voids, as shown in Fig. 7(c). The SSWM strip is wrapped on the circumference of the cylinder by keeping an overlap zone of 50 mm to ensure the proper bonding and avoid sliding or debonding of SSWM strips [32]. To prepare the smooth and level surface, the SSWM strip is covered with the final coat of Sikadur 30LP, with nearly 1 to 2 mm thick, as shown in Fig.7 (d).

(a) Grinded Cylinder (b) First layer of adhesive (c) Wrapping with SSWM (d) Final layer of adhesive

Figure 7: Strengthening Procedure of the Concrete Cylinder.

Test procedure and instrumentation

The experimental study on the cylinders is being conducted at the Heavy Structures Laboratory of Nirma University. The compression test for all the specimens is conducted using a hydraulic compression testing machine with a capacity of 3000 kN. Two steel plates on both end surfaces of the concrete cylinder are positioned in such a way as to achieve consistent loading. Load cell and LVDT are used to measure the load on specimens and deformation of the specimens, respectively, as shown in Fig. 8. The compressive load is applied at a rate of 4.04 kN/sec as per IS 516 – 2021 [24]. Two pairs of 5 mm electric resistance strain gauges have been attached to partially wrapped concrete cylinders. Fig. 6 shows two strain gauges, one strain gauge in the axial and the other in the circumferential direction. These strain gauges are mounted at the centre of SSWM strips in such a way that they are adequately spaced and away from the overlap zone to study the axial and hoop strain distribution of the SSWM strip as shown in Fig. 6 and Fig. 8. While fully SSWM-wrapped specimens and unconfined specimens, one pair of 90 mm electrical resistance strain gauges is mounted at the centre of the specimens, as shown in Fig. 8. A Data Taker DT80 system is utilised to record the measured quantities of various sensors such as load cell, LVDT, and strain gauges into a computer at every second, as shown in Fig. 8.

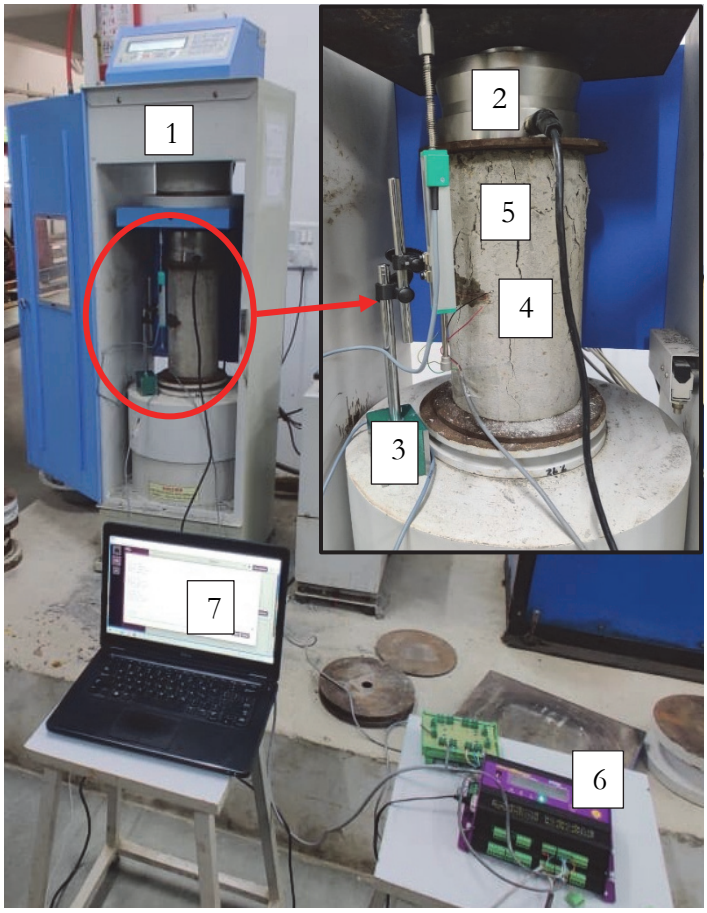

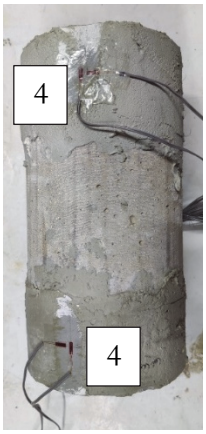

Location of Strain Gauge

1) Compression testing machine
2) Load cell
3) LVDT
4) Strain Gauges
5) Test specimen
6) Data Taker DT80
7) Laptop to receive data from Data Taker DT80 and store

Figure 8: Test Setup for Compression Test.

EXPERIMENTAL RESULTS AND DISCUSSION

The stress-strain behaviour and failure mode for the SSWM confined cylinders observed during the experiment are explained in subsequent sections. The specimen is categorised as a short column with a slenderness ratio of two, so that the slenderness does not affect the test results.

Axial compressive load vs. strain behaviour of specimens

The graph in Fig. 9 illustrates the relationship between axial compressive load and strain for both confined and unconfined concrete cylinders. Due to damage to a few strain gauges during testing, only one pair of strain gauge results for each

specimen is depicted in Fig. 9. Tab. 4 provides comprehensive test results for all specimens, presenting key parameters such as maximum axial load (P_u), maximum axial stress (f'_{cc}), and corresponding axial (ε_{cc}) and hoop (ε_{ru}) strains.

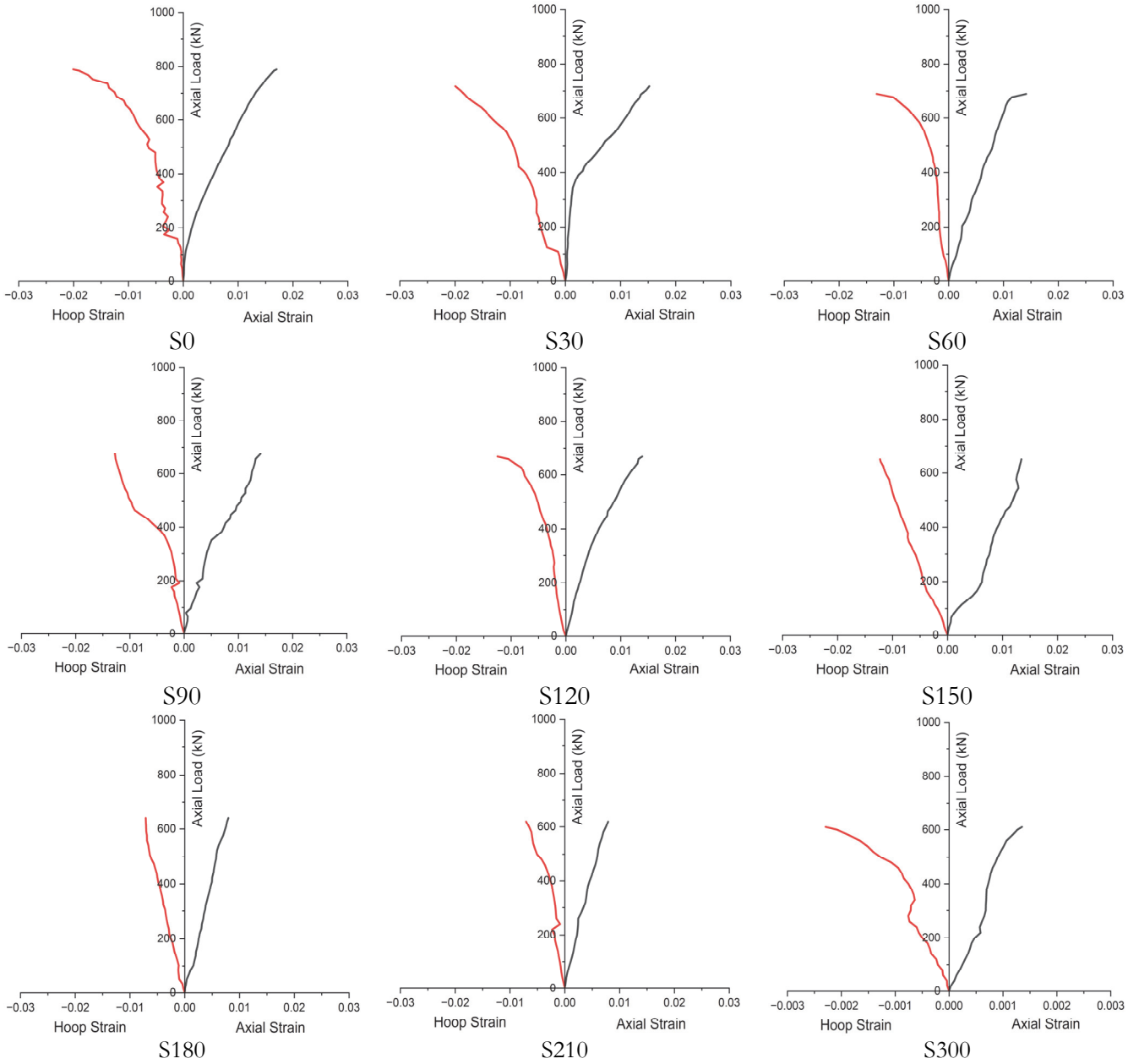

Figure 9: Behavior of axial load vs axial strain and hoop strain for test specimens.

As the gap between SSWM strips increases, there is a noticeable reduction in axial strain and circumferential strains in the wrapped region. This indicates a diminished ability of SSWM strips to provide effective confinement. Initially, the stress-strain responses of confined concrete mirror those of unconfined concrete. However, after reaching the strength of unconfined concrete, most specimens exhibit a strain-softening behaviour, ultimately demonstrating a nearly nonlinear response until ductile failure due to SSWM rupture. Strain-softening responses are observed when strip gaps are lower than the specimen diameter, signifying sufficient confinement and ductile behaviour. Additionally, when strip gaps surpass the specimen diameter, the effectiveness of confinement becomes negligible. This observation is supported by strain gauge readings corresponding to peak load with significant strip gaps ($S \geq 150$ mm), where axial and hoop strains of SSWM strips drastically decrease, indicating marginal confinement effectiveness. Tab. 4 shows that the average strains of SSWM confining strips at rupture are less than the rupture strain of the SSWM obtained from tensile coupon tests (Tab. 2). It demonstrates

that the strain capacity of the SSWM material is not fully utilised before the rupture. Two probable reasons to explain the observed strain inefficiency are the geometry of the confined concrete section and the small thickness of SSWM with negligible out-of-plane bending stiffness.

Partially confined concrete with SSWM exhibits a strain-hardening behaviour when the gap between the strips is equal to or less than 120 mm. Moreover, a narrower gap between the strips leads to a significant increase in peak load. Notably, specimens with strip gaps of 180 mm and 210 mm show strain distributions similar to unconfined concrete. These findings collectively highlight the dependency of SSWM effectiveness on the gap between confining strips, providing valuable insights into the response of partially confined with SSWM on concrete under axial load.

Specimen Identification	Peak Axial Load (kN) P_u	f'_{cc} (MPa)	f'_{cc}/f'_c	ε_{cc} (%)	$\varepsilon_{cc}/\varepsilon_c$	ε_{rw} (%)	$\varepsilon_{rw}/\varepsilon_{uss}$	Remarks
S300 (Control)	610	34.52	1	0.1353	0.68	--	--	Strain Gauge attached to Concrete Surface
S210	620	35.08	1.02	0.7909	3.95	-0.7074	-0.0557	
S180	641	36.27	1.05	0.7962	3.98	-0.7121	-0.0561	
S150	651	36.84	1.07	1.3418	6.71	-1.2287	-0.0967	
S120	668	37.80	1.10	1.3921	6.96	-1.2485	-0.0983	Strain Gauge attached to SSWM Surface
S90	675	38.20	1.11	1.4077	7.04	-1.2761	-0.1005	
S60	690	39.05	1.13	1.4128	7.06	-1.3151	-0.1036	
S30	717.5	40.60	1.18	1.5207	7.60	-1.9955	-0.1571	
S0	789	44.65	1.29	1.7015	8.51	-2.0081	-0.1581	

ε_c is cracking strain (considered as 0.2%) and ε_{uss} rupture strain of SSWM (considered as 12.7% as per Tab. 2)

Table 4: Comparison of axial compressive strength and strain of control and SSWM-strengthened specimens.

Failure modes

The failure characteristics of partially SSWM-wrapped confined concrete cylinders exhibit variations based on different gaps between confining strips, as illustrated in Fig. 10. Specimens that have full wrapping, as well as those with smaller strip gaps of 30 mm to 90 mm, experience failures because of SSWM rupture. On the other hand, specimens with strip gaps higher than 90 mm undergo initial failures due to the crushing of concrete in the unwrapped region of the specimen. During testing, inclined shear cracks are observed in specimens with strip gaps of 120 mm, 150 mm, and 180 mm. As the unconfined compressive strength is approached in partially wrapped specimens, unwrapped concrete begins to exhibit cracking and spalling. The crushing of concrete in the unwrapped region is insignificant for the specimens with smaller strip gaps of 30 mm and 60 mm, and it remains nearly intact even after post-failure of specimens. It appears that the SSWM strips offer adequate confinement to the unwrapped concrete. Conversely, specimens with strip gaps of 180 mm and 210 mm display concrete crushing, indicating minimal confinement effectiveness. The performance of partially SSWM-confined concrete diminishes significantly with an increasing gap between confining strips. Therefore, effective confinement is observable when the spacing is less than the diameter of the confined concrete. Even the experimental results also suggest that the SSWM confinement effect becomes negligible when the spacing exceeds the diameter of the confined concrete as per observation strain values, as shown in Tab. 4.

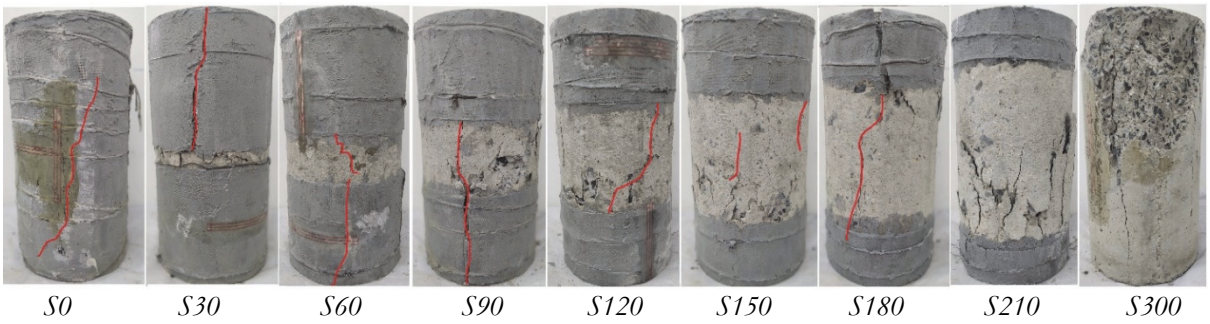

Figure 10: Failure mode of cylinders.

MECHANICS OF CONFINEMENT

The SSWM wrapping exerts a passive confinement action on the concrete cylinder, which occurs due to the lateral expansion of concrete under axial load. A uniform radial pressure created against the lateral expansion of SSWM-confined concrete develops the tensile hoop stress, which leads to an increase in axial stress and a corresponding increase in the lateral strain.

Confinement modulus and confinement strength

In addition to the inherent material properties of concrete, the performance of concrete is influenced by two key factors: confinement modulus and confinement strength. The confinement modulus, denoted as Cs and expressed in Eqn. 3, is defined as the ratio of the increment of confinement stress (Δf_r) to the radial strain $(\Delta \varepsilon_r)$, as illustrated in Fig. 11 [13].

$$C_s = -\frac{\Delta f_r}{\Delta \varepsilon_r} \tag{3}$$

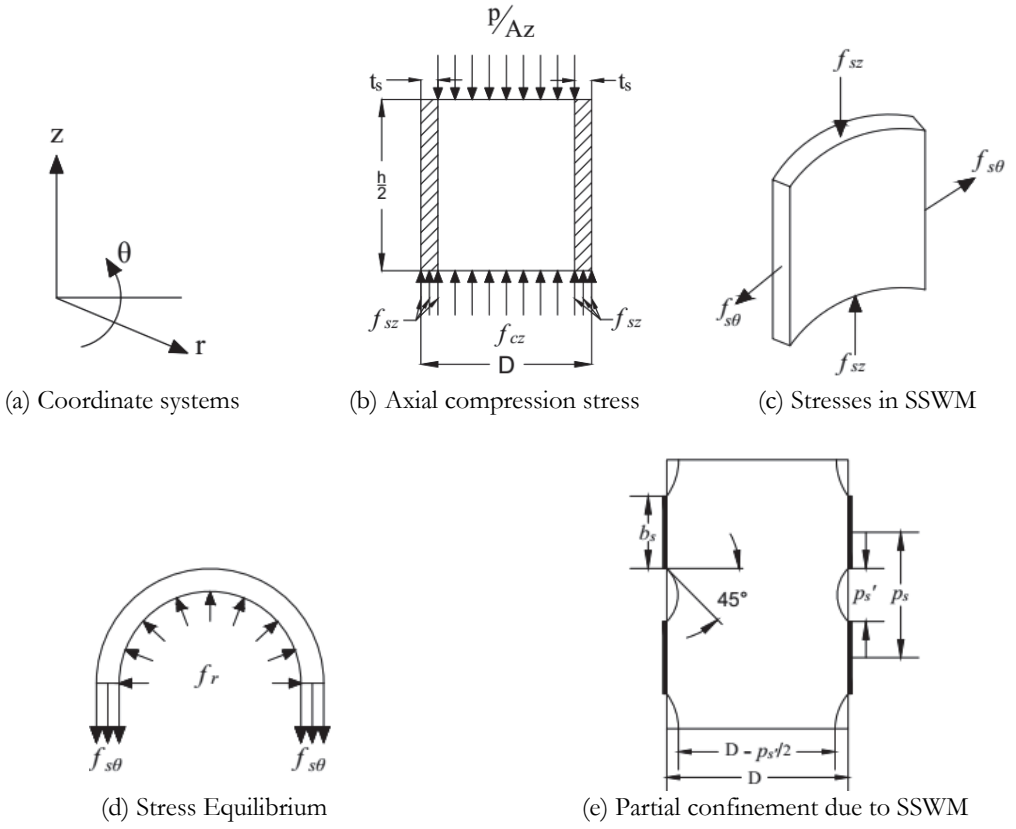

(a) Coordinate systems (b) Axial compression stress (c) Stresses in SSWM

(d) Stress Equilibrium (e) Partial confinement due to SSWM

Figure 11: Confinement mechanism.

The negative sign in the equation signifies passive confinement, indicating a negative work performed during lateral expansion deformation.
The following two equations can be derived from equilibrium condition and compatibility conditions as:

$$\varepsilon_r = \varepsilon_{s\theta} \tag{4}$$

$$f_r \times D = -f_{s\theta} \times t_s - f_{s\theta} \times t_s \tag{5}$$

$$f_r = -\frac{2t_s}{D} f_{s\theta} \tag{6}$$

where t_s = thickness of SSWM, $f_{s\theta}$ and $\varepsilon_{s\theta}$ = circumferential stress and strain of SSWM, respectively and D = diameter of the cylindrical concrete column.
From Eqn.3, 4 and 6, the confinement modulus can be written as given in Eqn. 7.

$$C_s = \frac{2t_s}{D} \frac{\Delta f_{s\theta}}{\Delta \varepsilon_{s\theta}} \tag{7}$$

Since the initial part of the stress-strain curve of SSWM is linearly elastic, so $\frac{\Delta f_{s\theta}}{\Delta \varepsilon_{s\theta}}$ can be assumed to be equal to Es of strengthening material. The constant confinement modulus, based on the thickness of SSWM, the diameter of the cylinder, and SSWM modulus, can be defined using Eqn. 8:

$$C_s = \frac{2\ t_s}{D} E_s \tag{8}$$

The confinement strength limit f_{ru} is determined by the ultimate strength of SSWM, denoted as f_{uss}, and is given by:

$$f_{ru} = \frac{2t_s}{D} f_{uss} \tag{9}$$

In general, confinement strength limit f_{ru} is determined by the geometric reinforcement ratio

$$f_{ru} = \frac{1}{2}\ \rho\, f_{uss} \tag{10}$$

The geometric reinforcement ratio (ρ) is calculated for the circular section as follows:

$$\rho = \frac{4\ t_s\ b_s}{D\ p_s} \tag{11}$$

where
t_s = thickness of SSWM,
b_s = height of SSWM strip,
p_s = c/c spacing of SSWM strip
D = diameter of circular section.
For continuous wrapping $\rho = \frac{4\ t_s}{D}$.

The geometric reinforcement ratio (ρ) as per CNR DT200 [13] and Mander et al. [33] for rectangular sections is given below:

$$\rho = \frac{2\, t_s\, b_s \left(b + h\right)}{b\, d\, p_s} \tag{12}$$

where b and h are the width and depth of the rectangular section.

The axial strain of concrete ε_{z} is determined based on LVDT reading. The axial and circumferential (hoop) strains of SSWM, denoted as ε_{sz} and $\varepsilon_{s\theta}$, are measured using electrical resistance strain gauges. Subsequently, the concrete strains ε_{cr} and $\varepsilon_{c\theta}$ are determined by applying the deformation compatibility condition within the cylinder section.

Despite the fact that SSWM itself does not directly bear the applied load, there is some axial stress present in SSWM due to the bonding between SSWM and concrete. To consider the indirect effect of strengthening, many models designed to predict the compressive strength of FRP-confined concrete columns rely on the general equation (Eqn. 13) proposed by Richart et al. [34]. This equation, initially developed for estimating the confined concrete with steel, has been adapted for FRP applications. Eqn. 13 is used for the present study to counteract the effect of SSWM on concrete compressive strength.

$$f_{cc}^{'} = f_{c}^{'} + k f_{lu} \tag{13}$$

where

$f_{cc}^{'}$ = Confiment compressive strength of concrete,

$f_{c}^{'}$ = Compressive strength of a plain concrete cylinder,

$f_{lu} = k_1 \times f_{ru}$ = Lateral confinement stress,

k_1 = Coefficient indicating the effectiveness of the SSWM confinement action.

Coefficient of efficiency k_1 is defined as a product of the horizontal (shape of confined section) coefficient (k_h), vertical (wrapping configuration of SSWM) coefficient (k_v) and inclination of SSWM with cross-section efficiency (k_α).

As per CNR DT200 [13] and Mander et al. [33] for the circular section $k_h = 1.0$, and for rectangular sections,

$$k_h = 1 - \frac{b^2 + h^2}{3\, A_g} \tag{14}$$

where A_g is the cross-section area, and b and h are the width and depth of the rectangular section. The coefficient k_v is dependent on the strengthening configuration along the longitudinal axis. For full wrapping configuration k_v =1, and for discontinuous wrapping configuration is considered as [35]:

$$k_v = \left(1 - \frac{p'_s}{2h}\right) \times \left(1 - \frac{p'_s}{2b}\right) \tag{15}$$

k_α depends on the inclination of the SSWM strip for the cross-section of the member and is defined as:

$$k_\alpha = \frac{1}{1 - (\tan\alpha)^2} \tag{16}$$

Eqn. 13 can be re-written as

$$f_{cc}^{'} = f_{c}^{'} + k k_h k_v k_\alpha f_{ru} \tag{17}$$

$$\text{SSWM confinement factor } (k_s) = \frac{f_{cc}^{'}}{f_c^{'}} = 1 + k k_h w_n \tag{18}$$

where,

$$w_n = k_v k_\alpha \rho \times \frac{f_{uss}}{2 f_c^{'}}$$

For the present study, using the proposed model given in Eqn. 18, the predicted confined compressive strength is calculated and plotted against the experimental confined compressive strength, as shown in Fig. 12. The figure indicates the good performance of the proposed model based on statistical data and Eqn. 19 is derived for the SSWM confinement factor (k_s).

$$k_s = 1 + 3.6 \times k_h w_n \tag{19}$$

A total of three categories of specimens are considered to assess the performance of the proposed model, as shown in Tab. 5 and Fig. 13. The accuracy is illustrated with the help of average absolute error (AAE) as well as mean square error (MSE) statistical indicators. The proposed model accurately predicts the peak strength for partially SSWM-confined concrete under direct compression load based on the performance of these statistical indicators. An illustration of the proposed model for the prediction of compressive strength of a partially SSWM-confined concrete cylinder with a strip gap of 30 mm is given in the Appendix.

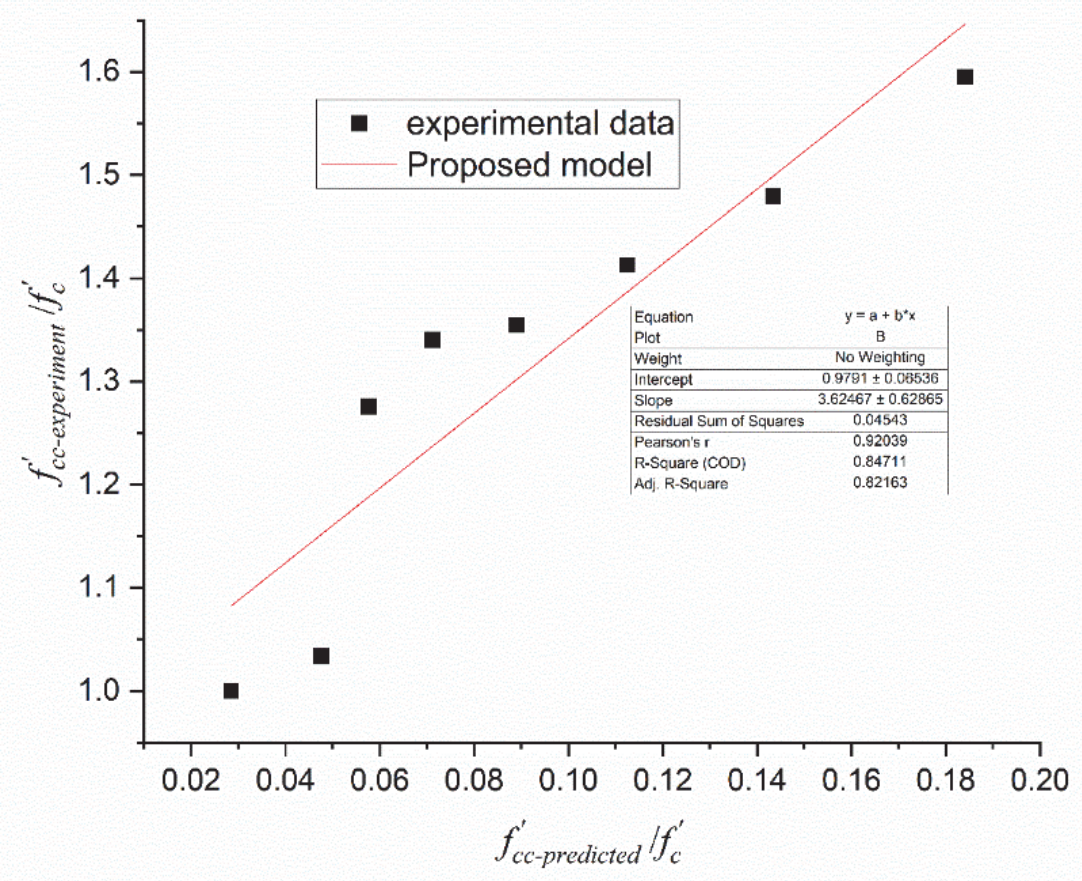

Figure 12: The proposed model based on the experimental data.

Specimen Identification	Experimental Results: Peak Axial Load (kN) P_u	Experimental Results: f'_{cc} (MPa)	Experimental Results: $\left(f'_{cc}/f'_c\right)_{Exp}$	Predicted Results: w_n	Predicted Results: $\left(f'_{cc}/f'_c\right)_{Pre}$	AAE: $\left\|\frac{\left(f'_{cc}/f'_c\right)_{Pre}-\left(f'_{cc}/f'_c\right)_{Exp}}{\left(f'_{cc}/f'_c\right)_{Exp}}\right\|$	MSE: $\left(\frac{\left(f'_{cc}/f'_c\right)_{Pre}-\left(f'_{cc}/f'_c\right)_{Exp}}{\left(f'_{cc}/f'_c\right)_{Exp}}\right)^2$	Remarks
S300 (Control)	610	34.52	1.00	0.00000	1.00	0.000031	0.000000	Present Experimental Study
S210	620	35.08	1.02	0.00251	1.01	0.007194	0.000060	
S180	641	36.27	1.05	0.00511	1.02	0.030811	0.000984	
S150	651	36.84	1.07	0.00913	1.03	0.032144	0.001070	
S120	668	37.80	1.10	0.01503	1.05	0.037388	0.001440	
S90	675	38.20	1.11	0.02341	1.08	0.020114	0.000428	
S60	690	39.05	1.13	0.03507	1.13	0.004301	0.000024	
S30	717.50	40.60	1.18	0.05111	1.18	0.006630	0.000037	
S0	789	44.65	1.29	0.07306	1.26	0.023493	0.000579	
C400M15W1	630	20.05	1.19	0.11206	1.40	0.180639	0.032631	Kumar and Patel [21]
C400M20W1	705	22.44	1.07	0.08998	1.32	0.239437	0.057330	
C400M25W1	920	29.28	1.18	0.07614	1.27	0.080220	0.006435	
40×32_1	770.50	43.6	1.26	0.07845	1.28	0.054982	0.000217	Patel et al. [32]
40×32_2	738.67	41.8	1.21	0.07845	1.28	0.014261	0.003416	
40×32_3	694.50	39.3	1.14	0.07845	1.28	0.048432	0.015817	
				$\sum_{1}^{N}\frac{AAE\ or\ MSL}{N}\times 100\ =$		**5.20%**	**2.31%**	

N is no. of specimens

Table 5: Performance of proposed model for ultimate strength prediction.

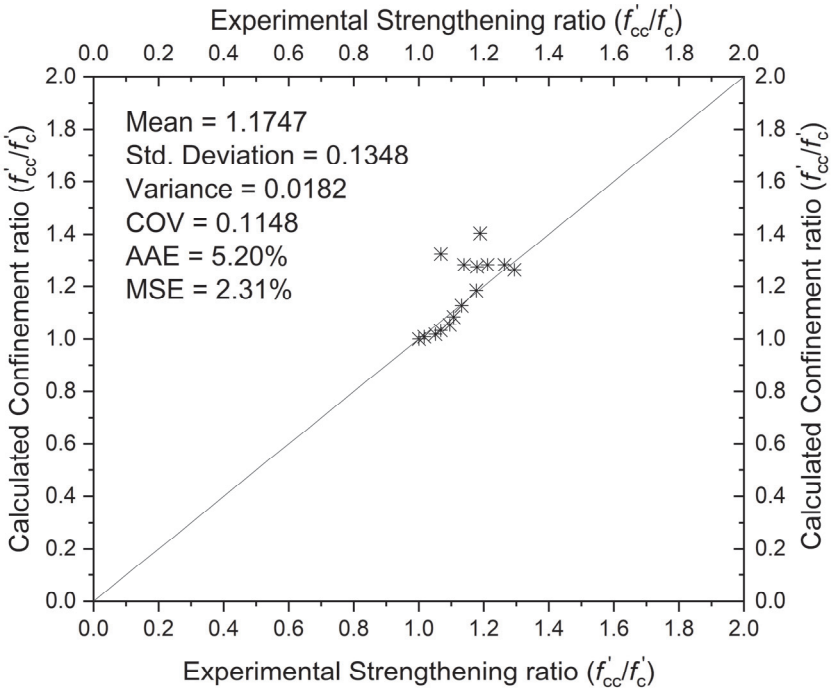

Figure 13: Performance of the proposed model for predicting confined compressive strength.

CONCLUSION

The experimental program outlined in the paper has provided crucial insights into the behaviour of SSWM-confined concrete. The enhancement in compressive stress and axial strain of concrete cylinders is contingent on the specific configuration of SSWM wrapping. The following conclusions are drawn to elucidate the effectiveness of SSWM wrapping on concrete:

- The strength and strain capacity of specimens wrapped with SSWM exhibit improvements compared to unconfined concrete cylinders. Fully wrapped concrete cylinder with SSWM (S0) exhibit improvements in strength by 29.35% as compared to an unconfined concrete cylinder. The enhancement in strength of a full-wrapped concrete cylinder (S0) is almost double than concrete cylinder wrapped with two strips of SSWM at 60 mm spacing (S60).
- Rupture of SSWM is observed in confined concrete when the gap between confining strips is less than the diameter of the cylinder. The ultimate strain in the SSWM wraps is notably lower than the rupture strain obtained from the tensile coupon test.
- The stress-strain response of SSWM-confined concrete cylinders can be characterised in two zones. The first zone is almost linear, reflecting the passive behaviour of SSWM. The second zone initiates with a transition and transforms into an active zone where SSWM functions as an active confining element.
- A novel and simplified model has been proposed, incorporating both the experimental results and the model available in CNR DT200 [13], to evaluate the compressive strength of SSWM-confined concrete. The conducted tests revealed a linear correlation between the strength of confined concrete and the pressure exerted by SSWM.
- The accuracy of the model is assessed with the help of average absolute error and mean square error, and results show nearly 5.20% and 2.31% error, respectively. It shows that the proposed model accurately predicts the peak strength for partially SSWM-confined concrete under compression load.

The purpose of the study to develop an analytical model for the compression behaviour of concrete with partial SSWM wrapping is achieved. The outcomes of the present study can be employed to develop an analytical model for the torsional behaviour of reinforced concrete beams strengthened with different wrapping configurations of Stainless Steel Wire mesh.

ACKNOWLEDGEMENT

This study is supported by the "TARE Scheme – Order # TAR/2020/000238" funded by the Science and Engineering Research Board (SERB), Department of Science & Technology, India. The authors would like to thank the funding agency for their generous support.

REFERENCES

[1] Jahami, A., Temsah, Y., Khatib, J. (2019). The efficiency of using CFRP as a strengthening technique for reinforced concrete beams subjected to blast loading, International Journal of Advanced Structural Engineering, 11(4), pp. 411–420. DOI: 10.1007/s40091-019-00242-w.

[2] Jahami, A., Temsah, Y., Khatib, J., Baalbaki, O., Kenai, S. (2021). The behavior of CFRP strengthened RC beams subjected to blast loading, Magazine of Civil Engineering, 103(3). DOI: 10.34910/MCE.103.9.

[3] Campione, G., Miraglia, N. (2003). Strength and strain capacities of concrete compression members reinforced with FRP, Cem Concr Compos, 25(1), pp. 31–41. DOI: 10.1016/S0958-9465(01)00048-8.

[4] Silva, M.A.G. (2011). Behavior of square and circular columns strengthened with aramidic or carbon fibers, Constr Build Mater, 25(8), pp. 3222–3228. DOI: 10.1016/J.CONBUILDMAT.2011.03.007.

[5] Wang, W., Sheikh, M.N., Al-Baali, A.Q., Hadi, M.N.S. (2018). Compressive behaviour of partially FRP confined concrete: Experimental observations and assessment of the stress-strain models, Constr Build Mater, 192, pp. 785–797. DOI: 10.1016/J.CONBUILDMAT.2018.10.105.

[6] Xiao, Y., Wu, H. (2000). Compressive Behavior of Concrete Confined by Carbon Fiber Composite Jackets, Journal of Materials in Civil Engineering, 12(2), pp. 139–146. DOI: 10.1061/(ASCE)0899-1561(2000)12:2(139).

[7] Ahmad, S.H., Shah, S.P. (1982). Stress-Strain Curves of Concrete Confined by Spiral Reinforcement, Journal Proceedings, 79(6), pp. 484–490. DOI: 10.14359/10922.

[8] Eid, R., Dancygier, A.N. (2006). Confinement effectiveness in circular concrete columns, Eng Struct, 28(13), pp. 1885–1896. DOI: 10.1016/J.ENGSTRUCT.2006.03.015.
[9] Eid, R., Dancygier, A.N., Paultre, P. (2007). Elastoplastic Confinement Model for Circular Concrete Columns, Journal of Structural Engineering, 133(12), pp. 1821–1831. DOI: 10.1061/(ASCE)0733-9445(2007)133:12(1821).
[10] Sundara Raja Iyengar, K.T., Desayi, P., Nagi Reddy, K. (2015). Stress-strain characteristics of concrete confined in steel binders, Magazine of Concrete Research, 22(72), pp. 173–184. DOI: 10.1680/MACR.1970.22.72.173.
[11] Martinez, S., Nilson, A.H., Slate, F.O. (1984). Spirally Reinforced High-Strength Concrete Columns, Journal Proceedings, 81(5), pp. 431–442. DOI: 10.14359/10693.
[12] Sheikh, S., Uzumeri, S.M. (1982). Analytical Model for Concrete Confinement in Tied Columns, Journal of the Structural Division, 108(12), pp. 2703–2722. DOI: 10.1061/JSDEAG.0006100.
[13] CNR-DT 200 R1. (2013). Guide for the Design and Construction of Externally Bonded FRP Systems for Strengthening Existing Structures Reliability of masonry building clusters.
[14] Lam, L., Teng, J.G. (2002). Strength Models for Fiber-Reinforced Plastic-Confined Concrete, Journal of Structural Engineering, 128(5), pp. 612–623. DOI: 10.1061/(ASCE)0733-9445(2002)128:5(612).
[15] De Lorenzis, L., Tepfers, R. (2003). Comparative Study of Models on Confinement of Concrete Cylinders with Fiber-Reinforced Polymer Composites, Journal of Composites for Construction, 7(3), pp. 219–237. DOI: 10.1061/(ASCE)1090-0268(2003)7:3(219).
[16] Micelli, F., Modarelli, R. (2013). Experimental and analytical study on properties affecting the behaviour of FRP-confined concrete, Compos B Eng, 45(1), pp. 1420–1431. DOI: 10.1016/j.compositesb.2012.09.055.
[17] Spoelstra, M.R., Monti, G. (1999). FRP-Confined Concrete Model, Journal of Composites for Construction, 3(3), pp. 143–150. DOI: 10.1061/(ASCE)1090-0268(1999)3:3(143).
[18] Vintzileou, E., Panagiotidou, E. (2008). An empirical model for predicting the mechanical properties of FRP-confined concrete, Constr Build Mater, 22(5), pp. 841–854. DOI: 10.1016/J.CONBUILDMAT.2006.12.009.
[19] Michel Samaan, B., Mirmiran, A., Shahawy, M. (1998). Model of Concrete Confined by Fiber Composites, Journal of Structural Engineering, 124(9), pp. 1025–1031. DOI: 10.1061/(ASCE)0733-9445(1998)124:9(1025).
[20] Teng, J.G., Lam, L. (2004). Behavior and Modeling of Fiber Reinforced Polymer-Confined Concrete, Journal of Structural Engineering, 130(11), pp. 1713–1723. DOI: 10.1061/(ASCE)0733-9445(2004)130:11(1713).
[21] Kumar, V., Patel, P.V. (2016). Strengthening of axially loaded circular concrete columns using stainless steel wire mesh (SSWM) – Experimental investigations, Constr Build Mater, 124, pp. 186–198. DOI: 10.1016/j.conbuildmat.2016.06.109.
[22] Kumar, V., Patel, P.V. (2016). Strengthening of axially loaded concrete columns using stainless steel wire mesh (SSWM)-numerical investigations, Structural Engineering and Mechanics, 60(6), pp. 979–999. DOI: 10.12989/sem.2016.60.6.979.
[23] IS 10262. (2019). Concrete Mix Proportioning - Guidelines, Bureau of Indian Standards, New Delhi.
[24] IS 516 (Part 1/Sec 1). (2021). Hardened Concrete-Methods of Test, Bureau of Indian Standards, New Delhi.
[25] Patel, P. V., Raiyani, S.D., Shah, P.J. (2018). Torsional strengthening of RC beams using stainless steel wire mesh - Experimental and numerical study, Structural Engineering and Mechanics, 67(4), pp. 391–401. DOI: 10.12989/sem.2018.67.4.391.
[26] Raiyani, S.D., Patel, P. V. (2023). Torsional strengthening of reinforced concrete hollow beams with stainless steel wire mesh, Proceedings of the Institution of Civil Engineers - Structures and Buildings, 176(8), pp. 584–600. DOI: 10.1680/jstbu.20.00126.
[27] Raiyani, S.D., Patel, P. V., Vora, S.D. (2020). Effectiveness of stainless steel wire mesh in shear strengthening of reinforced concrete flanged beam, International Journal of Structural Engineering, 10(3), pp. 195–216. DOI: 10.1504/IJSTRUCTE.2020.108525.
[28] Banaraswala Metal Crafts (P) Ltd. (2016). Woven Wire Cloth & Perforated Sheet Product Data Sheet, Banaraswala Metal Crafts (P) Ltd, Coimbatore. Available at: www.banaraswala.com.
[29] ASTM D3039/D3039M-17. (2017). Standard Test Method for Tensile Properties of Polymer Matrix Composite Materials, DOI: 10.1520/D3039_D3039M-17.
[30] Patel, P., Joshi, D., Makawana, R. (2023). Experimental studies to evaluate tensile and bond strength of Stainless-Steel Wire Mesh (SSWM), Frattura Ed Integrità Strutturale, 17(65), pp. 257–269. DOI: 10.3221/IGF-ESIS.65.17.
[31] Product Data Sheet, Adhesive for Bonding Reinforcement, version GCC, (Edition 10/09/2016, ID No.020401040010000003), Retrieved 21 - 10, 2016.
[32] Patel, P. V., Joshi, D.D., Makawana, R. V. (2023). Experimental studies on confined compressive strength of Stainless Steel Wire Mesh (SSWM) wrapped concrete columns, Mater Today Proc. DOI: 10.1016/j.matpr.2023.08.087.

[33] Mander, J.B., Priestley, M.J.N., Park, R. (1988). Theoretical Stress-Strain Model for Confined Concrete, Journal of Structural Engineering, 114(8), pp. 1804–1826. DOI: 10.1061/(ASCE)0733-9445(1988)114:8(1804).
[34] Richart, F.E., Brandtzæg, A., Brown, R.L. (1928). A study of the failure of concrete under combined compressive stresses, University of Illinois. Engineering Experiment Station. Bulletin ; No. 185.
[35] Chalioris, C.E. (2007). Analytical model for the torsional behaviour of reinforced concrete beams retrofitted with FRP materials, Eng Struct, 29(12), pp. 3263–3276. DOI: 10.1016/j.engstruct.2007.09.009.

APPENDIX

Compressive strength of partially SSWM-confined concrete cylinder example

Calculate the compressive strength of the partially SSWM-confined concrete cylinder with strip gaps of 30 mm in the middle of specimens, as shown in Fig. 6. The cylinder specimen size is 150 mm in diameter and 300 mm in height and is tested under compression load. The average compressive strength of a concrete cylinder at 28 days of curing is 34.52 MPa. In addition, 40 × 32 type SSWM with 0.27 mm wire diameter strengthens the concrete cylinder. The average ultimate tensile strength of SSWM is 700.16 MPa, as per Tab. 2.

Solution:
Step 1: Input parameters

Compressive strength of the cylinder ($f_c^{'}$) – 34.52 MPa
Depth of cylinder (h) – 300 mm
Width/diameter of the cylinder (b or D) – 150 mm
Spacing between SSWM strips (p'_s)– 30 mm
The thickness of SSWM – 0.27 mm
Ultimate tensile strength of SSWM (f_{uss}) – 700.16 MPa

Step 2: SSWM confined compressive strength of the cylinder

SSWM confined compressive strength of the cylinder can be predicted as per Eqn. 19

$$f_{cc}^{'} = f_c^{'} \times \left(1 + 3.6 \times k_h w_n\right)$$

$k_h = 1$ as per the CNR DT200 [6] for the circular section and $w_n = k_v k_\alpha \rho \times \frac{f_{uss}}{2 f_c^{'}}$

k_v is calculated as per Eqn. 15.

$$k_v = \left(1 - \frac{p'_s}{2h}\right) \times \left(1 - \frac{p'_s}{2b}\right) = \left(1 - \frac{30}{2 \times 300}\right) \times \left(1 - \frac{30}{2 \times 150}\right) = 0.855$$

k_α is calculated as per Eqn. 16 and k_α is dependent on the inclination of the SSWM strip on the cross-section of the member. SSWM is making zero-degree inclination with the cross-section of the cylinder therefore k_α is calculated as 1.

The geometric reinforcement ratio (ρ) is calculated as per Eqn. 11 for the circular section.

$$\rho = \frac{4\ t_s\ b_s}{D\ p_s}$$

b_s = height of SSWM strip = (Total height of cylinder – spacing between SSWM strip) /both ends of the cylinder
= (300 – 30)/2 = 135 mm

p_s = c/c spacing of SSWM strip = b_s + p'_s = 165 mm

$$\therefore \rho = \frac{4 \times 0.27 \times 135}{150 \times 165} = 0.00589$$

$$\therefore w_n = 0.855 \times 1 \times 0.00589 \times \frac{700.16}{2 \times 34.52} = 0.05107$$

and SSWM confined compressive strength of the cylinder can be calculated as

$$f'_{cc} = f'_c \times \left(1 + 3.6 \times k_b w_n\right) = 34.52 \times \left(1 + 3.6 \times 1 \times 0.05107\right) = 40.87 \text{ MPa.}$$

% increase in strength with respect to unstrengthened concrete cylinder = $\frac{40.87 - 34.52}{34.52} \times 100 = 18.38\%$